FARADAY

Near-UV photodissociation dynamics of formic acid

Stephen R. Langford, Alexander D. Batten, Mitsuhiko Kono† and Michael N. R. Ashfold*‡
School of Chemistry, University of Bristol, Bristol, UK BS8 1TS

H (Rydberg) atom photofragment translational spectroscopy has been used to study the photodissociation dynamics of jet-cooled formic acid molecules following excitation to their first excited singlet (S_1) state at numerous wavelengths in the range 216–241 nm. Analysis of the resulting H-atom time-of-flight spectra indicates contributions from three H-atom formation channels, which we identify as the primary C—H and O—H bond fission processes and the secondary photolysis of HCO($\tilde{X}$) fragments resulting from primary C—O bond fission. It also allows determination of the bond dissociation energies: D_0(H—CO_2H) ≈ 30 000 cm^{-1} and D_0(HCOO—H) = 39 080 ± 100 cm^{-1}. The former bond fission is deduced to occur after intersystem crossing to the neighbouring $\tilde{a}\,^3A''$ state, and to involve passage over (or tunnelling through) a barrier in the C—H dissociation coordinate on the triplet potential-energy surface. O—H bond fission, in contrast, is shown to occur predominantly on the S_1 surface but it, too, must overcome an activation barrier, the magnitude of which we can estimate at *ca.* 5400 cm^{-1}, measured relative to the asymptotic products H + HCOO($\tilde{X}$ and/or $\tilde{A}$). The latter assignment affords a refined value for the 0 K heat of formation of the formyloxyl radical: $\Delta_f H^\circ_0$ (HCOO) = −119.5 ± 3 kJ mol^{-1}.

Recent laser studies of the UV spectroscopy and photochemistry of formyl fluoride, HFCO, have led to major advances in our understanding of the fragmentation dynamics of this molecule following excitation to its first excited ($\tilde{A}\,^1A''$) singlet state. Specifically, a combination of jet-cooled parent spectroscopy (both parent-laser-induced fluorescence[1–3] and, at shorter wavelengths, measurements of the 'action' spectrum for forming H-atom photoproducts) and of the Doppler linewidths[2,3] and the times-of-flight[4,5] of these nascent H atoms, have shown the C—H bond fission process to occur *via* intersystem crossing (ISC) and subsequent dissociation on the lowest triplet potential-energy surface. Both the C—H and C—F bond-fission channels show activation barriers. The C—H bond-fission process in HFCO has been characterised at a number of excitation wavelengths in the range 218–248 nm, and the detailed energy partitioning into product rotation, vibration and translation, rationalised in terms of a hybrid model which allows both dynamical (associated with the forces acting as the dissociating molecule traverses the transition-state region associated with the barrier maximum) and statistical contributions to the overall energy disposal.[5]

Formic acid, HCO_2H, is isoelectronic with HFCO. The present work describes the results of a high-resolution photofragment translational spectroscopy (PTS) study of the various H-atom formation processes following near-UV excitation of HCO_2H, with a view to identifying similarities and differences between the photochemistry of these two molecules. The longest wavelength part of the electronic spectrum of HCO_2H shows resolved rovibronic structure,[6–9] the analysis of which confirms the $\tilde{A}\,^1A''(S_1)$–$\tilde{X}\,^1A'(S_0)$ transition symmetry and allows identification of the electronic origin at 37 431.5 cm^{-1} (267.2 nm).[7] Both the strength and the diffuseness of the absorption increase with decreasing wavelength. The cross-section appears to peak near 210 nm, whilst the structure merges to an apparent continuum at $\lambda \leqslant 200$ nm. The observed vibrational structure has been assigned in terms of progressions involving ν_3 (C=O stretch), ν_7 (O—C=O bend), and the out-of-plane motions ν_8 and ν_9.[6,7] Such vibrational activity is fully consistent with the assignment of this UV absorption system in terms of a $\pi_{C=O}^* \leftarrow n_O$ electronic promotion connecting the (planar) $\tilde{X}^1A'$ (S_0) ground state and an excited singlet state with a pyramidal equilibrium geometry in which both H atoms are twisted out of the plane defined by the O—C=O backbone, in an *anti*-configuration. Note that, although the excited state is non-planar, it is assumed to invert sufficiently easily that the A″ symmetry label is still applicable since the permutation group is isomorphous with C_s.[6]

The experimentally observed fluorescence lifetime of the S_1 origin level is *ca.* 50 ns,[10] some two orders of magnitude shorter than the radiative lifetime of comparable carbonyl molecules like H_2CO or HFCO. Possible competing non-radiative decay processes include internal conversion (IC) to high levels of the S_0 state, ISC to the neighbouring T_1 state arising from the same $\pi^* \leftarrow n$ excitation, and predissociation. Fragmentation routes that are energetically possible following excitation within the $\tilde{A}$–$\tilde{X}$ absorption system[10] include the molecular eliminations:

$$HCO_2H + h\nu \rightarrow H_2O + CO; \qquad \Delta H_0 \approx 35 \text{ kJ mol}^{-1} \quad (1)$$

$$\rightarrow H_2 + CO_2; \qquad \Delta H_0 \approx -6 \text{ kJ mol}^{-1} \quad (2)$$

process (3) leading to OH radical formation:

$$HCO_2H + h\nu \rightarrow HCO(\tilde{X}) + OH(X) \qquad \Delta H_0 \approx 452 \text{ kJ mol}^{-1} \quad (3)$$

and the two bond-fission channels leading to H-atom formation:

$$HCO_2H + h\nu \rightarrow H + CO_2H(\tilde{X}) \quad (4)$$

$$\rightarrow H + HCO_2(\tilde{X}) \quad (5)$$

The dynamics and the energetics of these two processes are major concerns of this paper, and are discussed in some detail later.

Brouard *et al.*,[8,10] have reported spectra showing the variation in OH(X) [and OH(A)] yield as a function of parent excitation wavelength. The electronically excited products are attributed to parent dissociation following two-photon absorption, resonance enhanced at the one-photon energy by

† Present address: Department of Pure and Applied Sciences, College of Arts and Sciences, University of Tokyo, Komaba, Meguro-Ku, Tokyo, 153 Japan.
‡ E-mail: mike.ashfold@bristol.ac.uk

the predissociating $\tilde{A}$ state. More relevant to the present work, the spectrum for forming ground-state OH products shows a long wavelength threshold at $\lambda \approx 252$ nm (some 2400 cm^{-1} above the S_1–S_0 origin) and gains in intensity with decreasing excitation wavelength. The quantum yield for channel (3) following excitation of HCO_2H at 222 nm has been estimated at $\Phi_3 \approx 0.8$.[11,12] Laser-induced fluorescence(LIF) and resonance-enhanced multiphoton ionisation (REMPI) probing of the OH(X) and HCO($\tilde{X}$) products, respectively, reveal both to be formed with little internal energy, with the bulk of any excess energy provided by the photolysis event appearing in the form of product recoil.[8,13–15] Intriguingly, the measured fluorescence lifetimes of $HCO_2H(\tilde{A})$ exhibit a clear decrease at slightly longer excitation wavelengths ($\lambda < 259$ nm, *ca.* 1200 cm^{-1} above the S_1–S_0 origin),[10] suggesting that at least one other dissociation channel is operating at energies below the appearance threshold of channel (3). A similar conclusion was reached by Abe and Hayashi,[9] in their wavelength-dependent study of $HCO_2H(\tilde{A}$–$\tilde{X})$ fluorescence quenching induced by an external magnetic field. This work clearly implicated ISC as one 'escape route' for $\tilde{A}$ state HCO_2H molecules but, to date, details of the dissociation mechanism (or mechanisms) has remained elusive. Finally, we note that previous end-product and radical scavenging experiments employing broad band ($\lambda > 220$ nm) photolysis[16] have suggested minor rôles for the H-atom loss channels (4) and (5), whilst studies of the thermal decomposition of ground-state formic acid in the temperature range 1370–2000 K show channel (1) to be the more important of the molecular eliminations.[17]

Here, we describe the results of high-resolution time-of-flight (TOF) measurements of the H-atom products arising in the photolysis of jet-cooled HCO_2H molecules following excitation at a number of wavelengths in the range 216–241 nm, each selected so as to correspond to a maximum in the excitation spectrum of the jet-cooled parent molecule.[18] These spectra provide new and detailed information about the relative importance, and the wavelength dependence, of fragmentation pathways (4) and (5), estimates of the respective H—C and H—O bond strengths, and some insight into the secondary photodissociation dynamics of HCO($\tilde{X}$) fragments formed in the primary step (3). The results are discussed in the light of previous knowledge concerning the photophysics of $\tilde{A}$ state HCO_2H molecules (summarised above) and our recent studies of $\tilde{A}$ state HFCO molecules.

Experimental

The H (Rydberg) atom PTS technique has been described previously.[19–23] A molecular beam of formic acid was prepared by bubbling Ar (*ca.* 1 atm pressure) through a sample of the liquid (Aldrich) held at *ca.* 310 K and introduced into the experiment *via* a pulsed nozzle (General Valve Series 9) mounted in its own diffusion-pumped chamber and thence, *via* a skimmer, into a cryopumped reaction chamber. Additional heating was supplied to the beam delivery tubing downstream of the formic acid reservoir to enhance the parent vapour pressure to *ca.* 70 Torr[24] and minimise dimerisation of formic acid and its condensation on the walls. The HCO_2H molecules are photolysed by one laser pulse (tuned to a parent absorption maximum in the wavelength range 216–241 nm), which crosses the molecular beam at right angles downstream from the skimmer, and the resulting H-atom photofragments are then 'tagged' using two laser pulses (at 121.57 nm and *ca.* 365.8 nm, respectively) propagating counter to the photolysis laser pulse to effect two-photon resonant excitation to a high-*n* Rydberg state. The necessary photolysis wavelengths were provided by a Nd-YAG pumped dye laser (Spectra-Physics GCR-270 plus PDL 2) operating on the dyes Coumarin 440, 460 and 480 with subsequent doubling of the dye laser output in a BBO crystal. The H atoms fly vertically a field-free distance of 425.6 mm along the third axis, orthogonal to the molecular beam and the laser beams, and are field ionised just prior to detection by a Johnston multiplier (type MM1-SG). The output from the multiplier is amplified and sent to a digital storage oscilloscope (LeCroy 9450, 350 MHz bandwidth) for display. The transient TOF spectrum thus obtained is then transferred to a computer (IBM PS-2) *via* a GPIB interface and the spectrum accumulated over, typically, 10^4 laser shots. Each data set is recorded at least three times and the TOF spectrum used in the subsequent data analysis is a sum of these replicates. Energy and momentum conservation allows conversion of the TOF spectra into total kinetic energy release (TKER) spectra.[22,23]

Results

TOF spectra of H atoms resulting from the photolysis of jet-cooled HCO_2H molecules were recorded at a total of twelve different excitation wavelengths in the range 216–241 nm. Fig. 1 shows spectra obtained at the two limiting wavelengths, 216.0 nm (46 282 cm^{-1}) and 240.86 nm (41 505 cm^{-1}) with the polarisation vector ε_{phot} of the photolysis laser aligned, respectively, perpendicular [(a) and (c)] and parallel [(b) and (d)] to the TOF axis. Clearly, at both wavelengths, the 'fast' and 'slow' H-atom peaks display different angular anisotropies, suggesting that (at least) two processes contribute to these spectra. All attempts to obtain spectra at $\lambda_{phot} > 241$ nm were thwarted by inadequate signal levels, reflecting, in part at least, the weak parent absorption at long wavelengths. Fig. 2 shows the corresponding TKER spectra, calculated assuming that the fragments partnering the observed H atoms have mass appropriate to the chemical formula CHO_2.

The 'fast' TOF peak, which is evident in all of the recorded spectra and shows with greater relative intensity when using higher photolysis pulse energies, maps into a broad, apparently continuous, spread of H-atom kinetic energies extending to very high TKER. We return to consider the origin of these fast H atoms later. Initially, we focus on the feature evident in Fig. 2 at low TKER. The spectra shown in Fig. 2(a) and (b) show a clear discontinuity at a TKER of *ca.* 7200 cm^{-1}. If we associate this with the threshold for a primary H—X bond-fission process such as (4) or (5) and further assume that, at the deduced onset, the partner fragment X is formed in its zero-point vibrational level, then energy conservation implies a bond dissociation energy $D_0(H—X) \approx 39\,100$ cm^{-1}. Fig. 3, which shows TKER spectra recorded at four intermediate wavelengths 219.25 nm (45 596 cm^{-1}), 222.86 nm (44 857 cm^{-1}), 224.86 nm (44 458 cm^{-1}) and 233.45 nm (42 823 cm^{-1}), provides support for such an interpretation. These TKER spectra each exhibit an apparently similar discontinuity at low TKER values, but more careful analysis reveals a subtlety. The onsets in the TKER spectra recorded at the shorter excitation wavelengths, *i.e.* at $\lambda_{phot} \leqslant 224.86$ nm, do indeed scale linearly with E_{phot} and are consistent with a mean bond dissociation energy of $39\,080 \pm 100$ cm^{-1}. TKER spectra recorded at longer excitation wavelengths show no obvious indication of this threshold, but do show a discontinuity at significantly higher TKER [*e.g.* a TKER of *ca.* 11 500 cm^{-1} in the case of Fig. 2(c) and (d)]. The poorer signal to noise ratio associated with spectra taken at the longer photolysis wavelengths makes determination of a precise onset difficult but, as Fig. 3 shows, it is possible to identify a second dissociation threshold at *ca.* 30 000 cm^{-1}. We recognise that these quoted values, derived on the basis that the observed thresholds correspond to formation of fragments with only zero-point internal energy, might well represent upper limits to the respective bond dissociation energies. Comparison with $D_0(H—OH) = 41\,250$ cm^{-1} [25] and $D_0(H—CHO) = 30\,285$ cm^{-1} [26] encourages association of these two thresholds with the HCOO—H [channel (5)] and H—CO_2H [channel (4)] bond-fission pro-

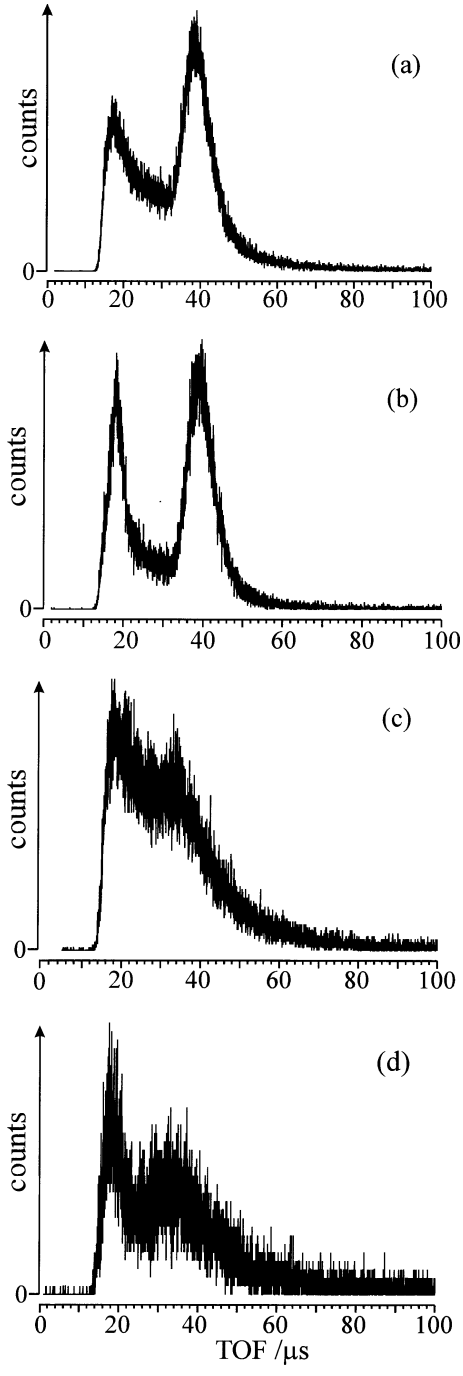

Fig. 1 TOF spectra of H atoms resulting from photolysis of jet-cooled HCO_2H molecules at 216.0 nm (46 282 cm^{-1}) [(a) and (b)] and 240.86 nm (41 505 cm^{-1}) [(c) and (d)]. The polarisation vector ε_{phot} was aligned, respectively, perpendicular [(a) and (c)] and parallel [(b) and (d)] to the TOF axis. Clearly, at both wavelengths, the 'fast' and 'slow' H-atom peaks display different angular anisotropies, suggesting that (at least) two processes contribute to these spectra.

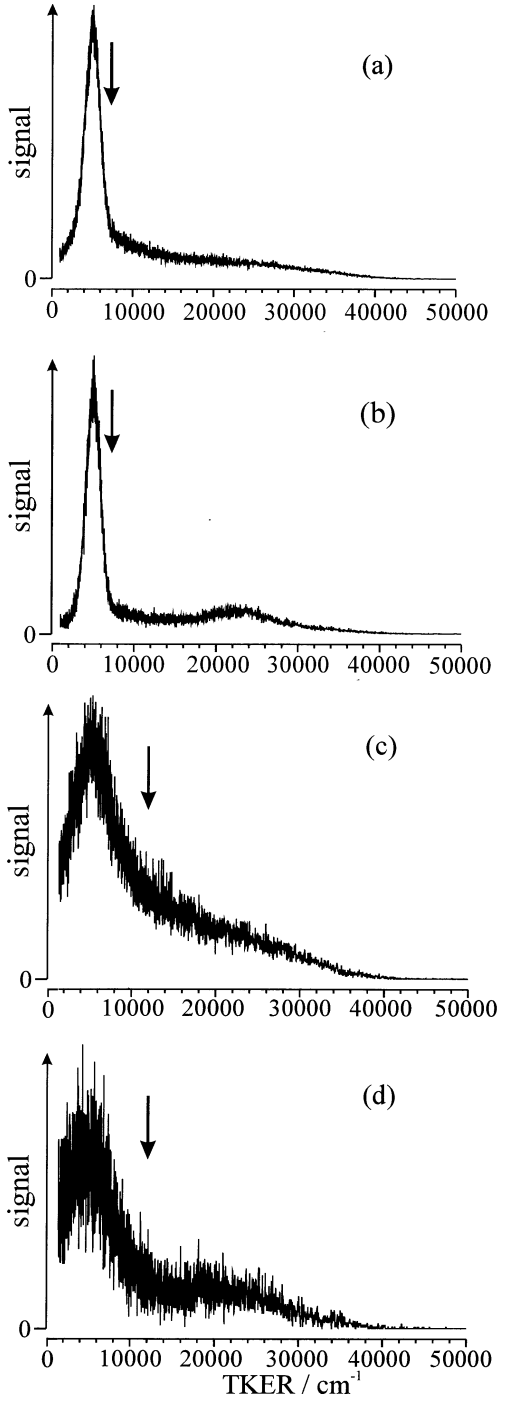

Fig. 2 TKER spectra derived from the TOF spectra shown in Fig. 1, calculated assuming that the fragments partnering the observed H atoms have a mass of 45.018 u (*i.e.* have the chemical formula HCO_2). The vertical arrows indicate the maximum TKERs for fragments associated with the O—H [(a) and (b)] and C—H [(c) and (d)] bond-fission channels, if we assume the bond dissociation energies given in the text.

cesses, respectively, but we reserve detailed consideration of this assignment till later.

Such an interpretation would imply that both O—H and C—H bond-fission processes contribute to the primary photochemistry of HCO_2H following excitation in the near UV. The proposed O—H bond fission is observed only at photolysis wavelengths, $\lambda_{phot} \leqslant 224.86$ nm. This photon energy exceeds the deduced D_0(HCOO—H) dissociation energy by some 5400 cm^{-1}, implying the presence of an activation barrier in the O—H exit channel. The maximum in the TKER distribution associated with these 'slow' H atoms and the shape of the fall-off at lower TKER are both consistent with a barrier of this magnitude and some tunnelling contribution to the H + HCO_2 yield.[5] H atoms attributable to C—H bond fission are clearly identified at longer photolysis wavelengths (Fig. 3). Since the implied D_0(H—CO_2H) is smaller than D_0(HCOO—H) it seems reasonable to assume that C—H bond fission also occurs at the shorter excitation wavelengths, but that its contribution to the TKER spectrum is obscured by the overlapping, sharper and more intense peak we attribute to O—H bond fission. The fact that the 'slow' H atom peak we associate with C—H bond fission also peaks well

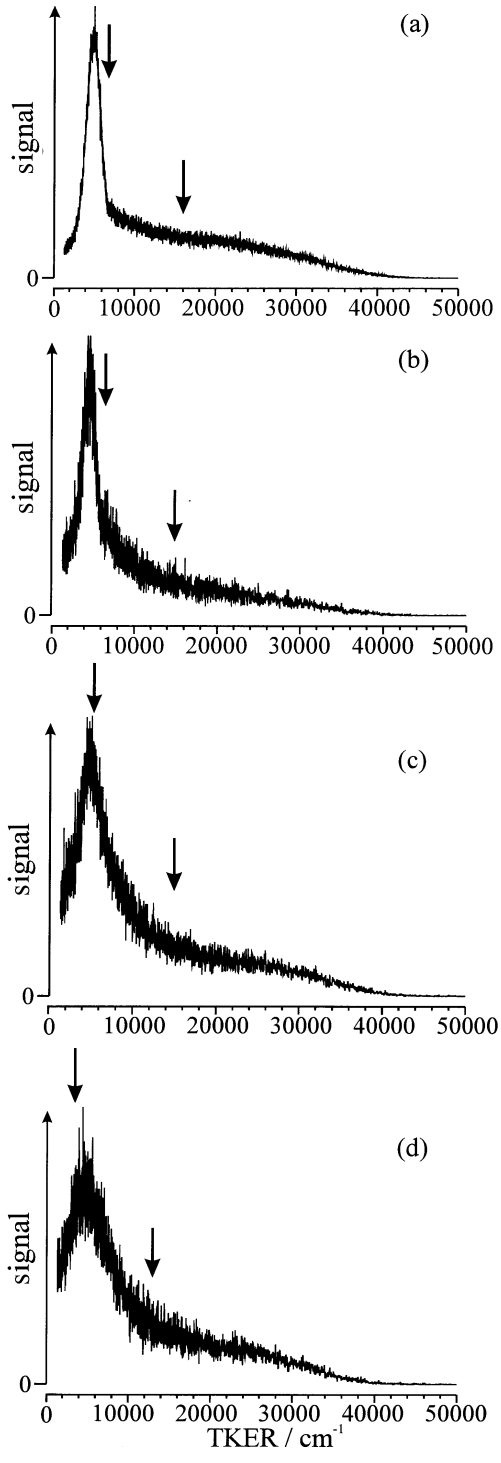

Fig. 3 TKER spectra obtained from linearly polarised photolysis (ε_{phot} perpendicular to the TOF axis) of jet-cooled HCO_2H molecules at (a) 219.25 nm (45 596 cm^{-1}), (b) 222.86 nm (44 857 cm^{-1}), (c) 224.86 nm (44 458 cm^{-1}) and (d) 233.45 nm (42 823 cm^{-1}). In each case the TOF → TKER conversion assumes that the observed H atoms are formed in conjunction with 'HCO_2' moieties. The vertical arrows indicate the maximum TKERs expected for products arising *via* O—H (lower TKER) and C—H (higher TKER) bond fissions, if we assume the bond strengths reported in the text.

above zero TKER suggests the presence of a (somewhat larger) activation barrier in this exit channel also.

The endothermicity of reaction (3) is established from the well defined enthalpies of formation: $\Delta_fH^\circ_0(OH) = 38.9$ kJ mol^{-1},[25] $\Delta_fH^\circ_0(HCO) = 41.4$ kJ mol^{-1} [26] and $\Delta_fH^\circ_0(HCO_2H) = -371$ kJ mol^{-1}.[27] These values, together with $\Delta_fH^\circ_0(H) = 216.0$ kJ mol^{-1} [25] and $\Delta_fH^\circ_0(CO_2H) = -220 \pm 3$ kJ mol^{-1},[27] imply a value of 367 ± 3 kJ mol^{-1} ($30\,700 \pm 250$ cm^{-1}) for the endoergicity of fragmentation (4). The good agreement between this value and the lower-energy dissociation threshold deduced in the present work validates our assignment of this threshold and serves to verify the internal consistency of the listed enthalpies. Kim *et al.*[28] have reported $\Delta_fH^\circ_0(HCO_2) = 126 \pm 13$ kJ mol^{-1}, from which we can predict $D_0(HCOO—H) = 461 \pm 13$ kJ mol^{-1} ($38\,540 \pm 1100$ cm^{-1}). As shown below, the accuracy with which we are able to define the threshold energy for O—H bond fission allows some refinement of $\Delta_fH^\circ_0(HCO_2)$.

Fig. 4 shows plots of the angular distributions of the 'fast' ($15 < t_H/\mu s < 19$), intermediate ($25 < t_H/\mu s < 28$) and 'slow' ($38 < t_H/\mu s < 42$) H-atom products resulting from photolysis of a jet-cooled sample of HCO_2H molecules at 216.0 nm (46 282 cm^{-1}). Following convention we attempt to fit these data in terms of the function[29]

$$I(v, \Theta) = (1/4\pi)f(v)[1 + \beta(\tfrac{3}{2}\cos^2\Theta - \tfrac{1}{2})] \quad (6)$$

where $f(v)$ is the speed distribution of the fragment, Θ is the angle between the $\boldsymbol{\varepsilon}$ vector of the photodissociation laser radiation and the velocity vector, $\boldsymbol{v}$, of the recoiling fragment, and β is the spatial anisotropy parameter. In the case of a prompt dissociation, β takes limiting values of $+2$, following excitation *via* a transition whose dipole moment μ lies in the plane of the molecule, and -1 when μ is perpendicular to the molecular plane. As Fig. 4 shows, the 'fast' and 'slow' H-atom yields both show angular distributions peaking at 0°, but exhibit different β parameters (0.9 ± 0.2 and 0.53 ± 0.15, respectively) which both fall far short of the limiting value $+2$, whilst the recoil velocity distribution for the 'intermediate' H atoms appears almost isotropic.

We now focus attention on the fast H-atom signal. One can envisage two possible explanations for these H atoms, the fastest of which appear with TKERs approaching that of the photolysis photon energy. One is two-photon dissociation of the parent molecule, such as has been invoked to account for the observed yield of electronically excited OH(A) fragments following excitation of HCO_2H at similar near-UV wavelengths.[8] The alternative is secondary photolysis of HCO($\tilde{X}$) fragments formed in the primary step (3). Fig. 5 shows two depictions of the fast parts of three different TKER spectra, plotted on energy scales appropriate to H atoms recoiling from partner fragments with masses of 45.018 u (HCO_2) and 28.01 u (CO), respectively. The onsets in the former, the left hand column in Fig. 5, show no obvious correlation with the

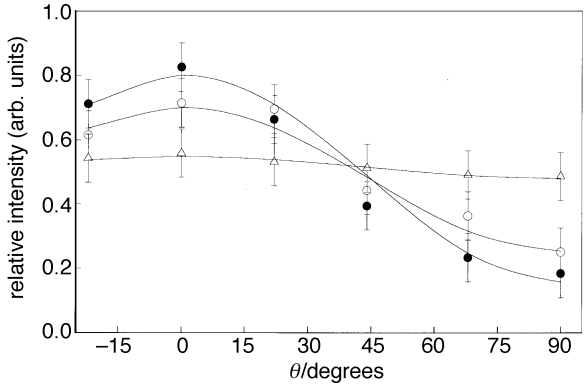

Fig. 4 Angular distributions of the 'fast' [(●) $15 < t_H/\mu s < 19$, $34\,600 > TKER/cm^{-1} > 21\,600$], intermediate [(△) $25 < t_H/\mu s < 28$, $12\,500 > TKER/cm^{-1} > 10\,000$] and 'slow' (○) $38 < t_H/\mu s < 42$, $5400 > TKER/cm^{-1} > 4400$] H-atom photofragments arising in the 216.0 nm (46 282 cm^{-1}) photolysis of a jet-cooled sample of HCO_2H. The points are experimental data; the curves are fits of $I(v, \Theta)$ in terms of eqn. (6). The best-fit β values are, respectively, 0.9 ± 0.2, 0.1 ± 0.1 and 0.53 ± 0.15.

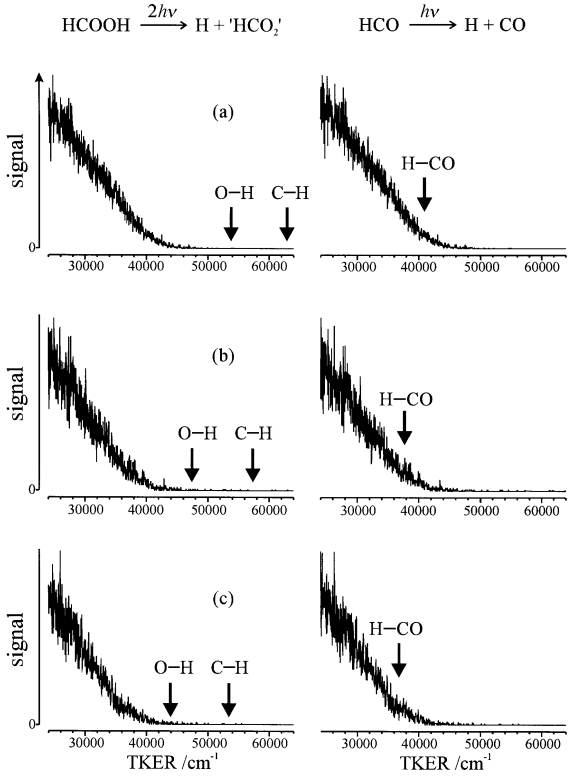

Fig. 5 'Fast' part of TKER spectra obtained from linearly polarised photolysis (ε_{phot} perpendicular to the TOF axis) of jet-cooled HCO_2H molecules at (a) 216.0 nm (46 282 cm^{-1}), (b) 230.0 nm (43 465 cm^{-1}) and (c) 240.86 nm (41 505 cm^{-1}). In each case, the TKER scale shown on the left-hand panel was derived assuming that the observed H atoms are formed in association with 'HCO_2' moieties, whilst the right-hand panel assumed the partner fragment to have a mass of 28.01 u (appropriate for CO). The vertical arrows in the left-hand panel indicate the maximum TKERs consistent with two-photon parent excitation followed by C—H and O—H bond fission to form ground-state products, whilst the arrow in each right-hand panel indicates the maximum TKER expected for fragmentation of stationary, internally cold HCO fragments.

calculated maximum possible TKER values associated with the bond fission processes (4) and (5). This, in itself, does not preclude the possibility that the fast signal arises from two-photon parent dissociation yielding H atoms together with internally excited 'HCO_2' moieties.

Such an interpretation appears unlikely, however, given the right-hand column of plots in Fig. 5, which reveal a good correlation between the observed onsets at high TKER and the maximum TKERs expected for secondary photolysis of HCO($\tilde{X}$) products. Such behaviour would be very reminiscent of that observed in the near-UV photolysis of the isoelectronic molecule HFCO.[5] These maximum TKERs indicated in the right-hand panel of Fig. 5 were calculated assuming D_0(H—CO) = 5300 cm^{-1},[30] and that the initial HCO fragments have no internal energy and zero velocity component along the TOF axis. In fact, previous studies of HCO_2H photolysis at 225 nm suggest that the HCO($\tilde{X}$) fragments arising *via* process (3) are created internally 'cold', but with mean translational energies of *ca.* 2000 cm^{-1} and a near-isotropic distribution of recoil velocity vectors.[8] This initial spread of HCO fragment velocities along the direction of the TOF axis provides a ready explanation for both the very fastest of the observed H atoms and the lack of structure in this fast part of the TKER spectrum. HCO is known to absorb throughout the relevant range of near-UV wavelengths,[31,32] and excited-state predissociation becomes important at excitation wavelengths shorter than 241 nm[33]. The anisotropy parameter measured here, $\beta = 0.9 \pm 0.2$, suggests that the dominant HCO absorption in the wavelength range 216–240 nm is associated with the parallel $\tilde{B}\,^2A'$–$\tilde{X}\,^2A'$ transition[31,32] and that the dissociation occurs rather promptly, whilst the broad spread of H atom TKERs suggests that the partner CO fragments are formed with a wide spread of internal energies. Franck–Condon considerations suggest that much of this excitation is likely to be in the form of CO vibration.

Discussion

The foregoing description suggests that both C—H and O—H bond-fission processes contribute to the primary photophysics of HCO_2H molecules following excitation within their S_1–S_0 absorption system, and allows a rather precise estimation of the respective dissociation energies. An additional yield of 'fast' H atoms is shown to arise from secondary photolysis of HCO($\tilde{X}$) fragments formed *via* the C—O bond-fission channel (3). We now attempt to rationalise these observations, and complementary findings from previous studies of the near-UV photochemistry of HCO_2H, in terms of relevant portions of the potential-energy surfaces for the ground and low-lying excited electronic states of this molecule. Our knowledge of these excited states is limited. Iwata and Morokuma[34] reported vertical excitation energies for the ground state and for the singlet and triplet excited states arising as a result of both $\pi^* \leftarrow n$ and $\pi^* \leftarrow \pi$ electron promotions. These suggest that the $^3A'$ state arising from the latter promotion might be the lowest-lying excited state, but that the corresponding $^1A'$ state lies so far above the $^3A''$ and $^1A''$ states arising from the $\pi^* \leftarrow n$ excitation to be of little relevance to the present study. However, they also emphasise the difficulty (at that time) of such triplet-state calculations and state that 'no definite conclusion on the relative order (of the triplet states) can be drawn from these calculations'. In what follows we begin by discussing the observed product yields, and their wavelength dependence, within a similar framework to that used when accounting for the UV photochemistry of HFCO,[2–5] *i.e.* simply in terms of the two excited states arising from the $\pi^* \leftarrow n$ excitation.

Symmetry arguments, analogous to those advanced in our recent considerations of the near-UV photochemistry of HFCO,[4,5] suggest that ground-state HCO_2H molecules correlate with the ground-state products $H + CO_2H(\tilde{X}\,^2A')$, whilst the photoexcited HCOOH($\tilde{A}\,^1A''$) molecules must correlate adiabatically with the lowest-energy excited set of products with overall symmetry A″. These correlations are shown schematically in Fig. 6. Lacking detailed *ab initio* or spectroscopic information on excited states of the CO_2H (HOCO) fragment, we presume, as in FCO, that they lie too high in energy to be relevant, given the excitation wavelengths used in the present studies and, consistent with existing thermochemical data, interpret the *ca.* 30 000 cm^{-1} dissociation energy as the threshold for forming ground-state $H + CO_2H$ products.

We can envisage two routes by which the initially prepared $HCO_2H(\tilde{A})$ molecules might dissociate to these ground-state products: IC to the parent ground state or ISC to the T_1 surface, followed in each case by subsequent unimolecular decay. The lowest rovibrational levels of the S_1 state fluoresce, but with a lifetime (*ca.* 50 ns) some one to two orders of magnitude shorter than the expected radiative lifetime.[10] This indicates that HCO_2H molecules, even in the zero-point level of the S_1 state, undergo some non-radiative decay process. The $S_1 \rightarrow S_0$ fluorescence intensity is observed to reduce in the presence of an external magnetic field.[9] This observation, and analogy with HFCO,[2–5] suggests that the predominant non-radiative decay route for HCO_2H molecules in the lowest rovibrational levels of the S_1 state is ISC to the T_1 state. C—H bond fission in HFCO involves passage over (or tunnelling through) an exit channel barrier on the T_1 potential-energy surface. This barrier has been rationalised in terms of a

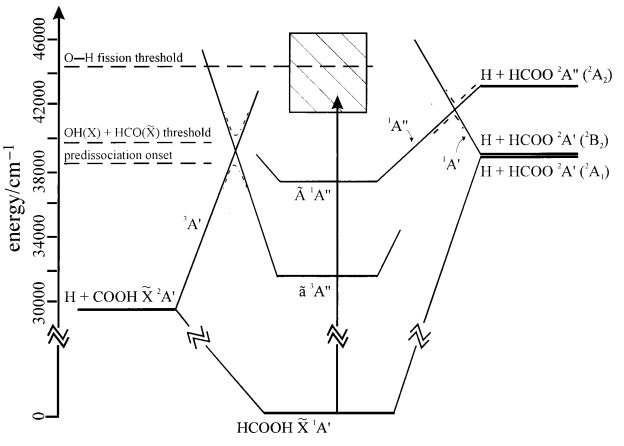

Fig. 6 Schematic correlation diagram for the fragmentation of HCO_2H molecules *via* C—H and O—H bond fission. The $\tilde{A}$–$\tilde{X}$ energy separation is determined from spectroscopy,[7] *ab initio* theory[34] provides an estimate of the singlet–triplet ($\tilde{A}$–$\tilde{a}$) splitting, and the present experiments provide the respective dissociation energies. Also indicated is the observed threshold for channel (3)[8] and (by the shaded box) the range of excitation energies investigated in the present work. Solid tie-lines show the parent → product correlations appropriate for C_s symmetries, whilst the dashed lines indicate the avoided crossings relevant to the present discussion that apply under the reduced (C_1) symmetry appropriate for non-planar configurations.

conical intersection between surfaces of ^{3}A" and ^{3}A' symmetry as shown in Fig. 6. Identification of a similar barrier in the H + CO_2H fragmentation channel would provide further confirmation of this proposed mechanism. Unfortunately, the present work indicates that D_0(H—CO_2H) lies well below the S_1–S_0 origin and, probably, below the T_1–S_0 origin[34] and this fact, combined with the weakness of the red end of the S_1–S_0 absorption in HCO_2H, prevented our making measurements at sufficiently long wavelength to establish the presence of such a barrier. It may be relevant to note, however, that the magnetic-field-induced fluorescence quenching studies of Abe and Hayashi[9] inferred the onset of a predissociation channel at excitation energies of *ca.* 38 600 cm^{-1}, below the appearance thresholds for fragmentation channels (3) and (5), which, by default, might be attributable to the onset of C—H bond fission. Such an interpretation would imply a barrier height of *ca.* 9000 cm^{-1} measured relative to the asymptotic products H + CO_2H; the breadth and the peak value of that part of the observed TKER spectra attributed to this channel implies that the CO_2H fragments are born with considerable internal energy. A barrier of this magnitude could also imply some role for IC and, as in HFCO,[3] for molecular product formation in the (slow) decay of HCO_2H molecules excited to the very lowest levels of the S_1 state.

Brouard *et al.*[8] have reported a long-wavelength threshold of *ca.* 252 nm (*ca.* 39 700 cm^{-1}) for forming OH(X) fragments *via* fragmentation channel (3). Such is consistent with our observation of secondary photolysis of the partner HCO($\tilde{X}$) fragment at all wavelengths investigated in the present work. This threshold energy exceeds the best thermochemical estimates of the reaction enthalpy by *ca.* 2000 cm^{-1}, thereby providing an estimate of the height of the energy barrier (again measured relative to the asymptotic products) in this exit channel. However, the mechanism of this particular dissociation pathway remains a matter of some debate. Scalar and vector properties of these OH(X) fragments have been investigated *via* measurements of the OH(A–X) LIF excitation spectrum, as a function of parent photolysis wavelength in the range 250–220 nm.[8,10,13,15] These studies reveal that: (i) the bulk of the available energy is partitioned into product translation, (ii) there is a slight preference for the OH(X) products to be formed in their Π^+(A') Λ-doublet state, (iii) there is little tendency for alignment of the angular momentum vector of the OH(X) fragments and (iv) the distribution of OH(X) fragment recoil velocity vectors is isotropic. These conclusions appear to be largely independent of the choice of photolysis wavelength or, therefore, of the precise vibronic composition of the initially prepared $HCO_2H(S_1)$ molecules.

All these observations would be consistent with a fragmentation process that occurs over a timescale that is long compared with the parent excited state vibrational (and rotational) period and, for this reason, Ebata *et al.*[13,15] favoured $S_1 \rightarrow S_0$ IC and subsequent dissociation on the ground-state surface as the likely fragmentation route. As in HFCO, however, there is no obvious reason why the ground-state potential-energy surface should exhibit a barrier in this bond-fission channel. For this reason, and because there is clear evidence that $S_1 \rightarrow T_1$ ISC is occurring at slightly lower excitation energies, it is worth considering whether this dissociation channel actually proceeds *via* the triplet surface. Indeed, given that $S_1 \rightarrow T_1$ ISC occurs and the fact that the T_1 surface should correlate with the ground-state OH + HCO products, the only reason why dissociation on the T_1 surface should not contribute to the observed OH(X) yield would be if the exit channel barrier is too high. However, the S_1 surface should also correlate with the ground-state OH + HCO products and Brouard *et al.*[8] have argued (by analogy with HONO[35–37]) that most (if not all) of the observed products actually arise *via* C—O bond fission on the S_1 surface and that the fragmentation timescale, the parent vibrational energy redistribution and the eventual energy disposal in the products are all manifestations of the detailed topology of this S_1 potential-energy surface. Such a view is supported by the quantum yield measurements,[11,12] which indicate channel (3) to be the dominant fragmentation route following photolysis at 222 nm. Careful study of parent absorption linewidths under jet-cooled conditions, and the way in which they vary with excitation energy, might provide evidence for the stepped reduction in excited-state lifetime that would be likely given the onset of such an adiabatic fragmentation route.

Finally, we consider the other observed primary X—H bond-fission channel, for which we propose an appearance threshold of *ca.* 224.85 nm, *ca.* 5400 cm^{-1} above the deduced bond dissociation energy. At this point we should mention the possibility that this substantial yield of slow H atoms is associated with C—H bond fission, leading to formation of electronically excited CO_2H fragments. Short of being able to confirm, or reject, the presence of an excited electronic state of the CO_2H fragment lying *ca.* 9000 cm^{-1} above the ground state, it is difficult to comment further on this possibility, but analogy with FCO suggests that such an explanation is unlikely.

Our favoured explanation involves the primary O—H bond-fission process (5). *Ab initio* theory[38] and experimental measurements of the photoelectron spectrum of HCO_2^- and DCO_2^- negative ions[28] reveal the near degeneracy of (and vibronic coupling between) the ground ($^2A_1$) and first excited ($^2B_2$) states of the formyloxyl radical, both of which have planar C_{2v} equilibrium geometries and both of which will transform as ^{2}A' in the distorted (C_s) point group. The second excited state, of $^2A_2$ symmetry (^{2}A" in C_s symmetry) lies only *ca.* 4300 cm^{-1} above the ground state.[28] The correlation diagram (Fig. 6) illustrates one way in which the experimental observations might be satisfied. The ground state of HCO_2H should correlate with the ground-state products H + $HCO_2(\tilde{X}\,^2A_1[^2A'])$, whilst the photoexcited $HCO_2H(\tilde{A}\,^1A'')$ molecules should correlate diabatically with the second excited asymptote H + $HCO_2(\tilde{B}\,^2A_2[^2A''])$. This latter correlation must be crossed by another tie-line linking the H + $HCO_2(\tilde{A}\,^2B_2[^2A'])$ products with a higher energy ^{1}A' state of HCO_2H (conceivably the ^{1}A' state arising from the $\pi^* \leftarrow \pi$ excitation). This crossing will manifest itself as a

conical intersection (with respect to the out-of-plane bend) between these two excited singlet potential-energy surfaces as shown in Fig. 6.

Thus, we propose that $HCO_2H(\tilde{A})$ molecules dissociate on the lower energy of these two excited-singlet adiabatic potential-energy surfaces, to yield $H + HCO_2$ products in their $\tilde{X}$ and/or $\tilde{A}$ states. Such a picture provides an explanation for: (i) the yield of these products relative to those attributable to the C—H bond-fission channel. No argument based on available phase space or product state densities, such as might apply if both fragmentations occurred on the T_1 surface, could accommodate such a large showing from this higher-energy product channel. (ii) The observed barrier in this exit channel, the actual magnitude of which will be influenced by the extent of configuration mixing as the molecule evolves along the O—H dissociation co-ordinate.

The comparative narrowness of this feature in the TKER spectrum suggests that most of the energy associated with the barrier to the $H + HCO_2$ back-reaction is released as product translation. The finding that these products exhibit a recoil velocity distribution characterised by a small positive β value is, at first sight, surprising, given the perpendicular nature of the S_1–S_0 transition. The likely explanation for this observation rests on the fact that the parent transition involves a pyramidal ← planar geometry change, the resulting S_1 molecules are therefore created with substantial out-of-plane bending motion (which may well be amplified by the conical intersection), which carries through into out-of-plane recoil of the H atoms.

Such a conclusion suggests that the value of Φ_3 measured at 222 nm,[11,12] just above the appearance threshold for channel (5), might well be close to its maximum and that future measurements at shorter excitation wavelengths might well show a decline as the alternative pathway (5) becomes increasingly competitive. It also allows determination of a refined value for the enthalpy of formation of the formyloxyl radical: $\Delta_f H_0^\circ(HCO_2) = -119.5 \pm 3$ kJ mol^{-1}, where the quoted error bounds allow for uncertainties both in the experimentally determined dissociation energy (± 1 kJ mol^{-1}), and in the exact value of $\Delta_f H_0^\circ(HCO_2H)$.

Conclusions

This work is concerned with fragmentation pathways leading to the formation of H atoms following photoexcitation of jet-cooled HCO_2H molecules in the wavelength range 216–241 nm. It complements previous studies of the OH(X) and, to a lesser extent, the $HCO(\tilde{X})$ fragments arising *via* the competing dissociation pathway (3).[8,10,13–15] We observe features attributable to primary O—H and C—H bond fission [channels (5) and (4), respectively] and to H atoms resulting from secondary photolysis of $HCO(\tilde{X})$ fragments arising *via* channel (3), and deduce dissociation energies for both of the primary bond fissions: $D_0(H—CO_2H) \approx 30\,000$ cm^{-1} and $D_0(HCOO—H) = 39\,080 \pm 100$ cm^{-1}. Consideration of all the available data, and comparison with recent photochemical investigations involving the isoelectronic molecule HFCO, suggests that HCO_2H molecules in their S_1 excited state decay *via* a number of competing decay pathways. C—H bond fission is an exoergic process for all levels of the S_1 state. As in HFCO, however, this process is deduced to occur on the triplet surface (accessed by ISC), and to involve passage over (or tunnelling through) an exit channel barrier. Two further fragmentation channels, (3) and then (5), open as we ascend in energy. Both are deduced to involve passage over exit channel barriers. Correlation arguments do not preclude either, or both, of these processes occurring on the triplet surface after ISC, but the observed dynamics and the deduced efficiencies of both fragmentation pathways encourage the assumption that both occur predominantly on the S_1 surface. Further insight into the photochemistry of formic acid, and the competition between the various possible non-radiative and dissociative decay channels available to $HCO_2H(S_1)$ molecules, should be provided by further PTS experiments involving the partially deuteriated species HCO_2D and DCO_2H, by *ab initio* calculations of relevant portions of the various excited-state potential-energy surfaces, by further high-resolution measurements of the jet-cooled $S_1 \leftarrow S_0$ excitation spectrum of HCO_2H (concentrating particularly on the variation of transition linewidth with excitation frequency) and by measurements of the wavelength dependence of the various product quantum yields.

Financial support from the EPSRC, NERC and the Royal Society is gratefully acknowledged, as is the advice and help of colleagues in Bristol (Prof. R. N. Dixon, C. L. Reed and K. N. Rosser), Oxford (Dr. M. Brouard) and Bielefeld, Germany (Prof. K. H. Welge and Dr. L. Schnieder). M. K. thanks the Japanese Society for the Promotion of Science for the award of a Postdoctoral Research Fellowship.

References

1 J. C. Crane, H. Nam, H. P. Beal, H. Clauberg, Y. S. Choi, C. B. Moore and J. F. Stanton, *J. Mol. Spectrosc.*, 1997, **181**, 56, and references therein.
2 R. N. Dixon and T. W. R. Hancock, *J. Phys. Chem.*, in press.
3 R. N. Dixon and T. W. R. Hancock, *J. Chem. Soc., Faraday Trans.*, 1997, **93**, 2707, and references therein.
4 C. L. Reed, M. Kono, S. R. Langford, T. W. R. Hancock, R. N. Dixon and M. N. R. Ashfold, *J. Chem. Phys.*, 1997, **106**, 6198.
5 C. L. Reed, M. Kono, S. R. Langford, R. N. Dixon and M. N. R. Ashfold, *J. Chem. Soc., Faraday Trans.*, 1997, **93**, 2721.
6 J. L. Ng and S. Bell, *J. Mol. Spectrosc.*, 1974, **50**, 166.
7 F. Ioannoni, D. C. Moule and D. J. Clouthier, *J. Phys. Chem.*, 1990, **94**, 2290.
8 M. Brouard, J. P. Simons and J-X. Wang, *Faraday Discuss. Chem. Soc.*, 1991, **91**, 63.
9 H. Abe and H. Hayashi, *J. Phys. Chem.*, 1994, **98**, 2729.
10 M. Brouard and J-X. Wang, *J. Chem. Soc., Faraday Trans.*, 1992, **88**, 3511.
11 G. S. Jolly, D. L. Singleton and G. Paraskevopoulos, *J. Phys. Chem.*, 1987, **91**, 3463.
12 D. L. Singleton, G. Paraskevopoulos and R. S. Irwin, *J. Phys. Chem.*, 1990, **94**, 695.
13 T. Ebata, A. Fujii, T. Amano and M. Ito, *J. Phys. Chem.*, 1987, **91**, 6095.
14 M. Brouard and J. O'Mahony, *Chem. Phys. Lett.*, 1988, **149**, 45.
15 T. Ebata, T. Amano and M. Ito, *J. Chem. Phys.*, 1989, **90**, 112.
16 R. Gorden, Jr. and P. J. Ausloos, *J. Phys. Chem.*, 1961, **65**, 1033, and references therein.
17 K. Saito, T. Kakumoto, H. Kuroda, S. Torii and A. Imamura, *J. Phys. Chem.*, 1984, **80**, 4989.
18 M. Brouard, personal communication.
19 L. Schnieder, W. Meier, K. H. Welge, M. N. R. Ashfold and C. M. Western, *J. Chem. Phys.*, 1990, **92**, 7027.
20 G. P. Morley, I. R. Lambert, M. N. R. Ashfold, K. N. Rosser and C. M. Western, *J. Chem. Phys.*, 1992, **97**, 3157.
21 D. H. Mordaunt, I. R. Lambert, G. P. Morley, M. N. R. Ashfold, R. N. Dixon, C. M. Western, L. Schnieder and K. H. Welge, *J. Chem. Phys.*, 1993, **98**, 2054.
22 S. H. S. Wilson, M. N. R. Ashfold and R. N. Dixon, *J. Chem. Phys.*, 1994, **101**, 7383.
23 M. N. R. Ashfold, D. H. Mordaunt and S. H. S. Wilson, *Adv. Photochem.*, 1996, **21**, 217.
24 D. R. Stull, *Ind. Eng. Chem.*, 1947, **39**, 517.
25 M. W. Chase Jr., C. A. Davis, J. R. Downey Jr., D. J. Frurip, R. A. McDonald and A. N. Syverud, JANAF Thermochemical Tables, *J. Phys. Chem. Ref. Data*, 1985, **14**, Supplement No. 1.
26 M-C. Chuang, M. F. Foltz and C. B. Moore, *J. Chem. Phys.*, 1987, **87**, 3855.
27 B. Ruscic, M. Schwarz and J. Berkowitz, *J. Chem. Phys.*, 1989, **91**, 6780.
28 E. H. Kim, S. E. Bradforth, D. W. Arnold, R. B. Metz and D. M. Neumark, *J. Chem. Phys.*, 1995, **103**, 7801.
29 R. N. Zare, *Angular Momentum*, Wiley, New York, 1988.
30 S. H. Kable, J-C. Loison, D. W. Neyer, P. L. Houston, I. Burak and R. N. Dixon, *J. Phys. Chem.*, 1991, **95**, 8013.

31 R. N. Dixon, *Trans. Faraday Soc*., 1969, **65**, 3141.
32 T. A. Cool and X. M. Song, *J. Chem. Phys*., 1992, **96**, 8675.
33 Y. J. Shiu and I. C. Chen, *J. Mol. Spectrosc*., 1994, **165**, 457.
34 S. Iwata and K. Morokuma, *Theor. Chim. Acta*., 1977, **44**, 324.
35 R. Vasudev, R. N. Zare and R. N. Dixon, *J. Chem. Phys*., 1984, **80**, 4863.
36 R. N. Dixon and H. Rieley, *J. Chem. Phys*., 1989, **91**, 2308.
37 R. Vasudev, S. J. Wategaonkar, S. J. Novicki and J. H. Shan, *A.C.S. Symp. Ser*., 1992, **502**, 279, and references therein.
38 A. Rauk, D. Yu, P. Borowski and B. Roos, *Chem. Phys*., 1995, **197**, 73, and references therein.

Paper 7/04119E; *Received* 12*th June*, 1997